Plant Physiology and Biochemistry 139 (2019) 293–306

Contents lists available at ScienceDirect

Plant Physiology and Biochemistry

journal homepage: www.elsevier.com/locate/plaphy

Research article

Functional analysis of the Chloroplast GrpE (CGE) proteins from *Arabidopsis thaliana*

L.A. de Luna-Valdez, C.I. Villaseñor-Salmerón, E. Cordoba, R. Vera-Estrella, P. León-Mejía, A.A. Guevara-García*

Departamento de Biología Molecular de Plantas, Instituto de Biotecnología, Universidad Nacional Autónoma de México, Av. Universidad 2001, Col. Chamilpa, Cuernavaca, Morelos, CP 62210, Mexico

ARTICLE INFO

Keywords:
Chloroplast
Chaperones
Cochaperones
Arabidopsis
GrpE
Hsp70

ABSTRACT

The function of proteins depends on specific partners that regulate protein folding, degradation and protein-protein interactions, such partners are the chaperones and cochaperones. In chloroplasts, proteins belonging to several families of chaperones have been identified: chaperonins (Cpn60s), Hsp90s (Hsp90-5/Hsp90C), Hsp100s (Hsp93/ClpC) and Hsp70s (cpHsc70s). Several lines of evidence have demonstrated that cpHsc70 chaperones are involved in molecular processes like protein import, protein folding and oligomer formation that impact important physiological aspects in plants such as thermotolerance and thylakoid biogenesis. Despite the vast amount of data existing around the function of cpHcp70s chaperones, very little attention has been paid to the roles of DnaJ and GrpE cochaperones in the chloroplast. In this study, we performed a phylogenetic analysis of the chloroplastic GrpE (CGE) proteins from 71 species. Based on their phylogenetic relationships and on a motif enrichment analysis, we propose a classification system for land plants' CGEs, which include two independent groups with specific primary structure traits. Furthermore, using *in vivo* assays we determined that the two CGEs from *A. thaliana* (AtCGEs) complement the mutant phenotype displayed by a knockout *E. coli* strain defective in the bacterial grpE gene. Moreover, we determined *in planta* that the two AtCGEs are *bona fide* chloroplastic proteins, which form the essential homodimers needed to establish direct physical interactions with the cpHsc70-1 chaperone. Finally, we found evidence suggesting that AtCGE1 is involved in specific physiological phenomena in *A. thaliana*, such as the chloroplastic response to heat stress, and the correct oligomerization of the photosynthesis-related LHCII complex.

1. Introduction

Chloroplasts are photosynthetic organelles of endosymbiotic origin that contain their own genome (Martin et al., 1998), which encodes 130 genes in average (RefSeq:https://www.ncbi.nlm.nih.gov/genome/organelle/). Estimations indicate that functional chloroplasts require 2000 to 3500 proteins (van Wijk and Baginsky, 2011), however the chloroplast genome codes for an average of only 83 proteins (RefSeq:https://www.ncbi.nlm.nih.gov/genome/organelle/). The rest of the chloroplastic proteome is encoded in the nuclear genome; using the cellular transcription and translation apparatus such proteins are synthesized in the cytoplasm and post-translationally imported into the organelle (Villarejo et al., 2005; Jarvis and Kessler, 2014; Paila et al., 2015). From their synthesis, chloroplast proteins are subjected to regulatory events that impact the performance of their functions; targeting, folding, post-translational stabilization, and degradation are processes that affect the homeostasis of chloroplast proteins (Trösch et al., 2015); these processes are regulated by molecular chaperones. In the cytoplasm, precursor proteins interact with the Hsp70, 14-3-3 and Hsp90 chaperones that keep them in a proper folding state and facilitate their interaction with the translocon receptor proteins Toc159 and Toc34 (Rial et al., 2000, May and Soll, 2000; Qbadou et al., 2006; Flores-Pérez and Jarvis, 2013).

In the chloroplast stroma, several chaperone systems have been identified. The chaperonins (Cpn60α and Cpn60β) are involved in the folding of RbcL (Ribulose Bisphosphate Carboxylase/Oxygenase large chain) and NdhH (NAD(P)H-quinone oxidoreductase subunit H) (Barraclough and Ellis, 1980; Peng et al., 2011), Hsp90s mediate protein import, protein maturation and thylakoid formation (Pratt and Toft, 2003; Heide et al., 2009; Inoue et al., 2013), Hsp100s prevent

* Corresponding author.
E-mail addresses: ldeluna@ibt.unam.mx (L.A. de Luna-Valdez), carlos.i.villasenor@gmail.com (C.I. Villaseñor-Salmerón), eliza@ibt.unam.mx (E. Cordoba), rosario@ibt.unam.m (R. Vera-Estrella), patricia@ibt.unam.mx (P. León-Mejía), aguevara@ibt.unam.mx (A.A. Guevara-García).

https://doi.org/10.1016/j.plaphy.2019.03.027
Received 8 December 2018; Received in revised form 26 February 2019; Accepted 17 March 2019
Available online 20 March 2019
0981-9428/ © 2019 Elsevier Masson SAS. All rights reserved.

Nomenclature

A. thaliana CGEs	AtCGEs
BiFC	Bimolecular Fluorescence Complementation
RbcL	Ribulose Bisphosphate Carboxylase/Oxygenase large chain
CGEs	chloroplast GrpE proteins
CrCGE1	C. reinhardtii CGE1
cYFP	Yellow Fluorescent Protein C-terminus
DXS	1-deoxy-D-xylulose-5-phosphate synthase)
Hip	Hsp70 interacting protein
Hop	Hsp70-Hsp90-organizing protein
NdhH	NAD(P)H-quinone oxidoreductase subunit H
nYFP	Yellow Fluorescent Protein N-terminus
pCE	pSPYCE vector
pD14	pDEST14 vector
pD22	pDEST22 vector
pD32	pDEST32 vector
pEG	pEarleyGate103 vector
pNE	pSPYNE vector
TCA	Trichloroacetic acid
VIPP1	Vesicle-inducing Protein in Plastids 1

protein aggregation and facilitate protein import and degradation (Kovacheva et al., 2007; Doyle and Wickner, 2009; Olinares et al., 2011; Clarke, 2012; Sjogren et al., 2014), and Hsp70s (cpHsc70-1 and cpHsc70-2) participate in thylakoid formation, protein import and photosystem assembly (Yalovsky et al., 1992; Schroda et al., 1999; Liu et al., 2007; Su and Li, 2008; Shi and Theg, 2010; Su and Li, 2010).

Mutant plants defective in chloroplast chaperones display pigment-defective phenotypes and contain aberrant chloroplasts. For example, *Arabidopsis thaliana* mutants in Cpn60α display albino phenotypes with impaired growth (Apuya et al., 2001), and point mutations in the Hsp90-5 gene also generate albino seedlings while null mutants are embryo-lethal (Cao et al., 2003; Inoue et al., 2013). The knockout of the major isoform of Hps93/ClpC causes chloroplast development and protein import defects (Constan et al., 2004; Kovacheva et al., 2005, 2007). Finally, mutation of cpHsc70-1 gene causes cotyledon and leaf variegation with chloroplast protein import defects, and double mutants for the two plastidic Hsc70s are embryo lethal (Su and Li, 2008).

To function efficiently, chaperones interact with other proteins known as cochaperones (Fink, 1999; Mayer, 2010). In chloroplasts, the cochaperonins Cpn10 and Cpn20 form hetero-oligomeric complexes to form the lid of the Cpn60 barrel-shaped oligomer (Tsai et al., 2012). Also, the C-terminus of Tic40 has homology to the proteins Hip (Hsp70 interacting protein) and Hop (Hsp70-Hsp90-organizing protein), which are known cochaperones that bind and organize Hsp70 and Hsp90 in the cytoplasm (Stahl et al., 1999; Bédard et al., 2007). In accordance, Tic40 has been found to directly interact with Hsp93/ClpC to enhance ATP hydrolysis (Chou et al., 2003).

Additionally, other cochaperones have been identified in chloroplasts, including DnaJ and GrpE domain-containing proteins. In *Escherichia coli,* such cochaperones directly interact with DnaK (Hsp70) to mediate protein folding. DnaJ is known to recruit target proteins and enhance the ATP hydrolysis of DnaK, while GrpE is a nucleotide exchange factor that regulates the exchange of ADP to ATP in the nucleotide-binding site of DnaK, thus regulating the affinity of the chaperone for the unfolded polypeptides (Fink, 1999; Mayer, 2010). In plastids, 19 DnaJ domain-containing proteins have been identified (Chiu et al., 2013), recent studies have found that mutant plants defective in individual DnaJ proteins (AtJ8, AtJ11, and AtJ20) display defects in PSII (Photosystem II) homeostasis in *A. thaliana* (Chen et al., 2010). Also, AtJ20 was found involved in the turnover of DXS (1-deoxy-D-xylulose-5-phosphate synthase) enzyme in *A. thaliana* (Pulido et al., 2013), whereas the DnaJ-containing protein CDJ2 from *Chlamydomonas reinhardtii* is required for the formation of the essential VIPP1 (Vesicle-inducing Protein in Plastids 1) oligomers during thylakoid biogenesis (Liu et al., 2005, 2007).

In contrast, the information regarding the function of the chloroplast GrpE proteins (CGEs) is fragmentary, with a comprehensive description available only for the *C. reinhardtii* CGE1. It is known that the CGE1 from *C. reinhardtii* is localized in the chloroplast stroma, where it interacts with HSP70B (the chloroplastic Hsp70 from *C. reinhardtii*), forms homodimers and participates in both protein import and VIPP1 oligomerization (Schroda et al., 2001; Liu et al., 2007; Willmund et al., 2007). Additionally, in *Physcomitrella patens* CGE proteins are localized in the chloroplast, where they interact with the stromal Hsp70-2

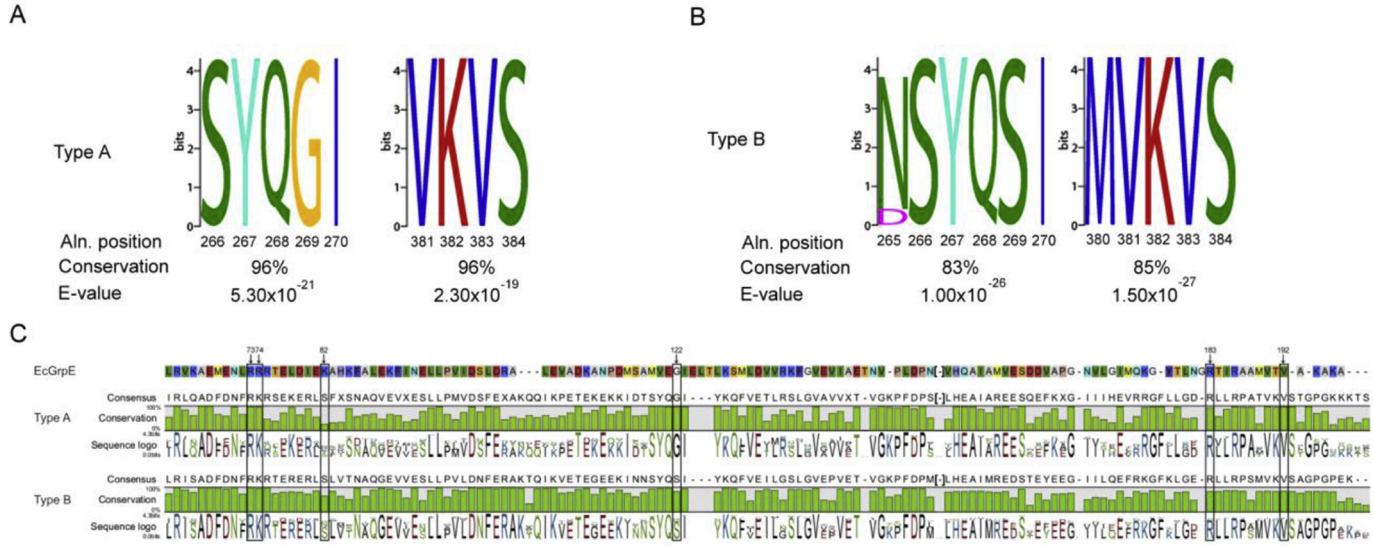

Fig. 1. Conserved motifs in CGE proteins. Sequence motifs found enriched in Type A (A) and Type B (B) CGEs based on the analysis with DREME tool (http://meme-suite.org/doc/dreme.html?man_type=web). The input sequences were randomized to generate a control set, the E-value threshold for motif discovery was set to 0.05. Alignment between the *E. coli* GrpE and the consensus sequences of Type A and Type B CGEs is shown (C). The numbers, arrows and boxes over positions 73, 74, 82, 122, 183, and 192 point to the amino acids that have been shown to be important for GrpE activity in *E. coli*.

protein to regulate protein import into the organelle (Shi and Theg, 2010). However, no experimental evidence exists that analyzes CGE function from land plants. This study presents data that gives insight into the functional traits of the *A. thaliana* CGEs, it is focused on the *in vivo* determination of several CGE protein traits that are relevant to its proposed function as a cochaperones for cpHsc70-1 protein, such as activity as nucleotide exchange factor, subcellular localization, physical interaction with cpHsc70 and dimer formation, it also presents information regarding the biological processes mediated by CGEs in *A. thaliana*.

2. Results

2.1. CGE proteins share functionally-relevant amino acid residues

To gain understanding of the evolution of CGEs, we performed a phylogenetic analysis of 136 CGE protein sequences from 71 species (61 embryophytes: 60 tracheophytes and 1 bryophyte, 7 chlorophytes, 1 charophyte, and 1 cryptophyte) (Fig. S1). A full alignment between all the analyzed CGEs and the *E. coli* GrpE is shown in the supplemental file CGEs full alignment. This analysis showed that the CGE protein sequences from embryophytes form a monophyletic group that further dives into two subgroups, named Type A and Type B. Analysis of the phylogenetic tree showed that 57% of the plants contain both Type A and Type B CGEs, while 18% contain only Type A and 24% only Type B CGEs. The two subgroups of CGEs can be distinguished from each other by variations in short motifs conserved in the analyzed CGE protein sequences. The SYQGI and VKVS motifs are present in Type A CGEs, and the (N/D)SYQSI and MVKVS are characteristic of Type B sequences (Fig. 1A and B). Furthermore, sequence comparison with the *E. coli* GrpE showed that two of the six amino acid positions essential for GrpE activity (Harrison et al., 1997; Gelinas et al., 2003, 2004) have been modified in the plant sequences. In embryophytes, amino acid position R74 was substituted by a K residue, and position K82 by an S residue (Fig. 1C and Table S2). Moreover, the G residue at position 122 of the *E. coli* GrpE is only conserved in Type A CGEs, while it has been substituted by S in 86% of the Type B CGEs (Fig. 1C and Table S2). The remaining functionally-relevant amino acids (R73, R183, and V192) from the bacterial GrpE are fully conserved among all the CGEs analyzed (Fig. 1C and Table S2). Finally, we observed that the two *CGE* genes present in the genome of *A. thaliana* belong to each of the two subgroups; *CGE2* to Type A and *CGE1/EMB1241* to Type B.

2.2. A. thaliana type A and type B CGEs are functional nucleotide exchange factors

To assess the functionality of the *A. thaliana* CGEs (AtCGEs), *AtCGE1* and *AtCGE2* genes were used to complement an *E. coli* knockout line (OD212) that is defective in the *grpE* gene. This mutant carries an additional mutation the Hsp70 gene (*dnaK332*) that suppresses the lethal phenotype conferred by the knockout of the endogenous *grpE*. Thus, OD212 line can grow normally at 25 °C but has growth defects when cultured at higher temperatures (Deloche et al., 1997). The predicted transit peptides were deleted from the CDSs of *AtCGE1* and *AtCGE2* genes, and the Shine-Dalgarno sequence was added to the genetic constructs to facilitate bacterial translation; the chimeric genes were cloned into the pDEST14 bacterial expression vector, generating the constructs *pD14::ΔCGE1* and *pD14::ΔCGE2* (Fig. S2). These constructs were transformed into OD212 cells and their phenotype was evaluated under permissive (25 °C), mild (37 °C), and restrictive (43 °C) temperature conditions (Fig. 2). The empty *pD14::ΔccdB* vector was used as negative control and the full lenght CDS of the *E. coli grpE* gene was cloned into pDEST14 and used as positive control (*pD14::EcgrpE*). Under permissive conditions, no detectable differences in growth were observed between the OD212 strain transformed with the empty vector and those carrying *pD14::ΔCGE1*, *pD14::ΔCGE2* and *pD14::EcgrpE* plasmids (Fig. 2). However, under mild temperature conditions (37 °C) improved growth was observed in the cells containing *pD14::ΔCGE1*, *pD14::ΔCGE2* and *pD14::EcgrpE* plasmids compared with the empty vector (Fig. 2). At the restrictive conditions (43 °C), the growth defects displayed by all the strains were more severe; however, cells transformed with *pD14::ΔCGE1*, *pD14::ΔCGE2* and *pD14::EcgrpE* plasmids performed better than the empty vector-transformed cells (Fig. 2). Furthermore, *pD14::CGE2*-carrying cells displayed improved growth compared with those containing *pD14::CGE1* (Fig. 2), indicating a better complementation capacity for *AtCGE2* compared to *AtCGE1*. These results demonstrate that the AtCGEs alleviate the defective phenotype of the OD212 mutant; supporting the idea that both AtCGEs retain key molecular traits that allow interaction with DnaK, to promote the essential nucleotide exchange needed by this chaperone.

2.3. A. thaliana CGEs are chloroplast localized

To investigate the role of CGEs as cochaperones for chloroplastic Hsp70s, their subcellular localization was determined *in vivo* and contrasted to the localization of the chloroplastic Hsp70, the cpHsc70-1 protein. Translational fusions of AtCGE1, AtCGE2, and cpHsc70-1 to

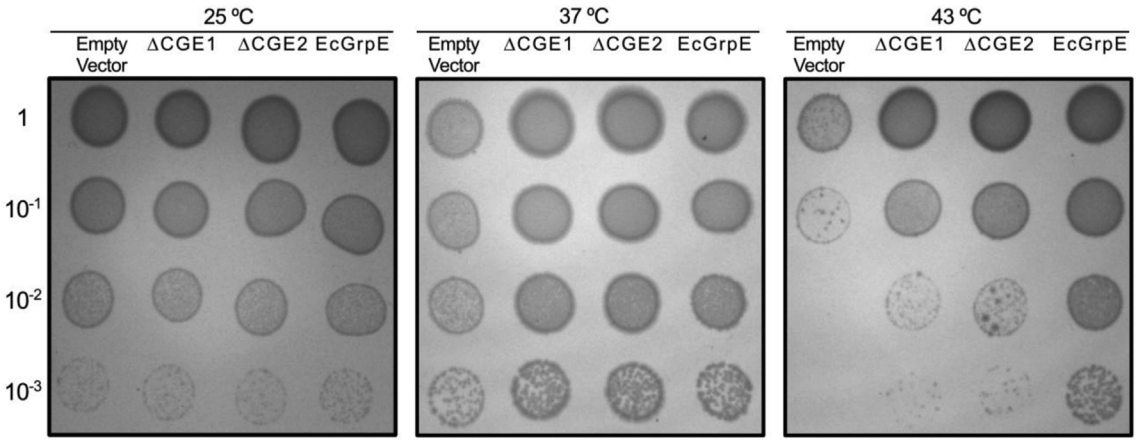

Fig. 2. Functional complementation assay in bacteria. The growth of the thermo-sensitive *E. coli* OD212 strain, transformed with the pD14:Δ*ccdB* (empty vector) or the expression vectors pD14:Δ*CGE1* (Δ*CGE1*), pD14:Δ*CGE2* (Δ*CGE2*) or pD14:*EcgrpE* (EcGrpE), was analyzed at 25 °C (A), 37 °C (B), and 43 °C (C). Five μL drops from the indicated bacterial samples were cultured for 20 h in LB-agar plates at the corresponding dilutions (1, OD_{600nm} = 0.1; 10^{-1}, OD_{600nm} = 0.01; 10^{-2}, OD_{600nm} = 0.001; 10^{-3}, OD_{600nm} = 0.0001) and temperature conditions.

GFP and c-Myc tag were generated (Fig. S2) and used to transform *N. benthamiana* leaves. Protoplasts from transformed leaves were analyzed 96 h post-transformation under the confocal microscope. The protoplasts expressing AtCGE1-GFP (Fig. 3B) or AtCGE2-GFP (Fig. 3C) fusions displayed GFP fluorescence distributed inside the chloroplast stroma and in discrete cumuli at the periphery of plastids. The formation of peripheral fluorescence cumuli has been described as chloroplast envelope deformations caused by overaccumulation of membrane-associated proteins (Breuers et al., 2012). Interestingly, protoplasts expressing cpHsc70-1-GFP fusion displayed a distribution pattern characteristic of stromal proteins (Fig. 3D), with intense fluorescence in a few foci inside the organelle (Farmaki et al., 2006; Perello et al., 2016). Additionally, we addressed the possibility of AtCGEs being transported to mitochondria by colocalization analysis of AtCGE1-GFP and AtCGE2-GFP and a translational fusion between mCherry and the yeast mitochondrial protein COX4 (Cytochrome c oxidase subunit 4) (Nelson et al., 2007), but no co-localization was found (Fig. S5). Altogether, these data indicate that both AtCGEs are *in vivo* imported into the chloroplast, where they coexist with cpHsc70-1 chaperone.

To confirm our data and to determine the suborganellar localization of the AtCGEs and cpHsc70-1 proteins, chloroplasts from *N. benthamiana* leaves transformed with *pNE::CGE1*, *pNE::CGE2* or *pNE::CPHSC70-1* constructs were isolated and fractionated into stromal and envelope fractions. Western blot analysis of purified suborganellar fractions was carried out using the c-Myc epitope tag present in the *pNE* expression vectors (Fig. S2). Fig. 4 shows that AtCGE1 and AtCGE2 proteins accumulate in both the chloroplast envelope and in the stromal fractions (Fig. 4: lanes 3 and 5), while cpHsc70-1 protein was only detected in the stromal fractions (Fig. 4 stromal fractions: lanes 2 and 4). Western blots against RbcS (stromal protein marker) and Tic40

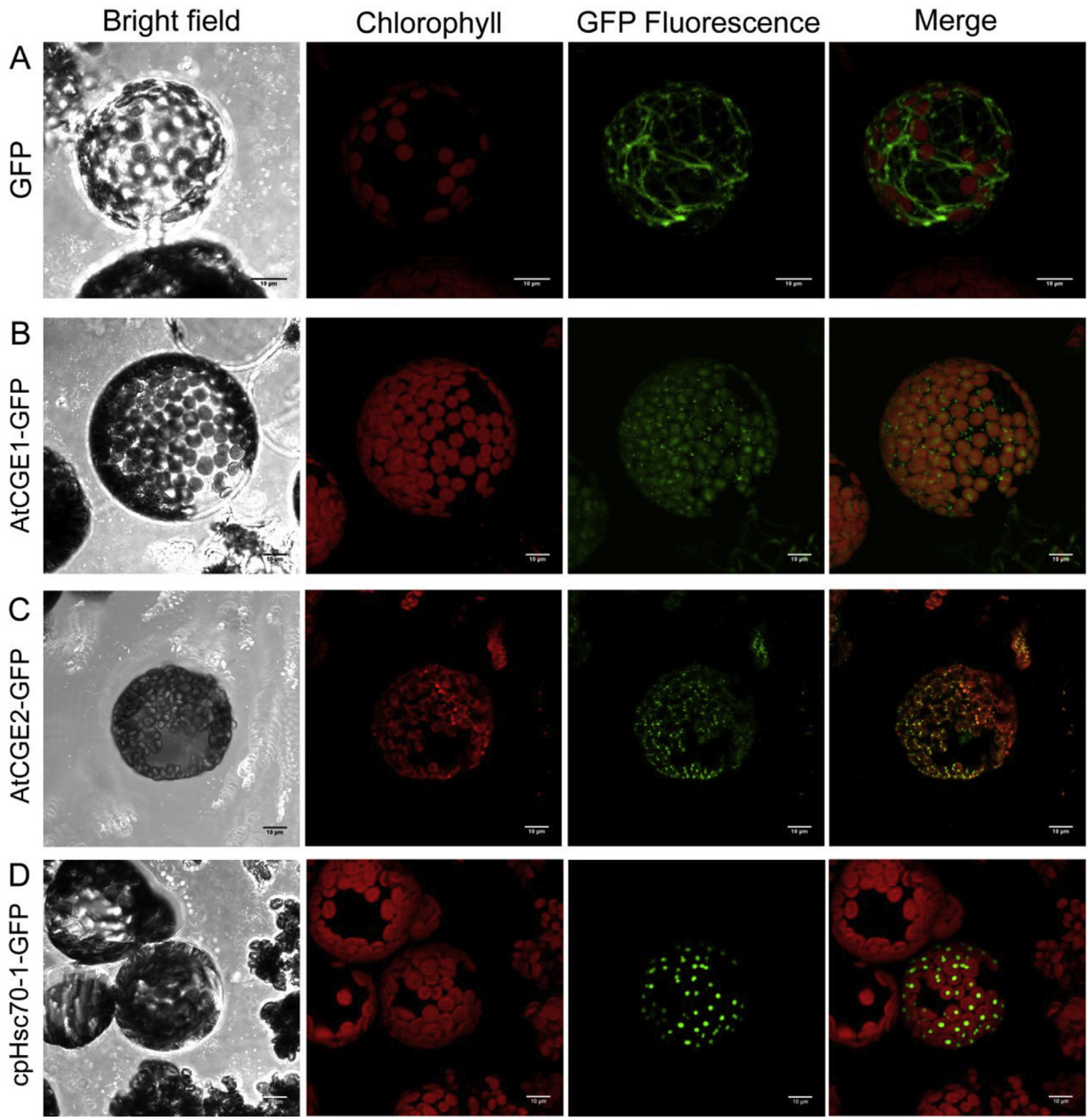

Fig. 3. Subcellular localization of AtCGE1, AtCGE2 and cpHsc70–1 proteins. Images of mesophyll protoplasts from *N. benthamiana* leaves expressing GFP (A) and the translational fusions AtCGE1-GFP (B), AtCGE2-GFP (C), and cpHsc70-1-GFP (D) are shown. Images corresponding to the bright field, chlorophyll fluorescence (Chlorophyll), GFP fluorescence, and the merge between the two fluorescence channels are shown in the indicated columns. Protoplasts were prepared 96 h after leaf agroinfiltration. Scale bars correspond to 10 μm.

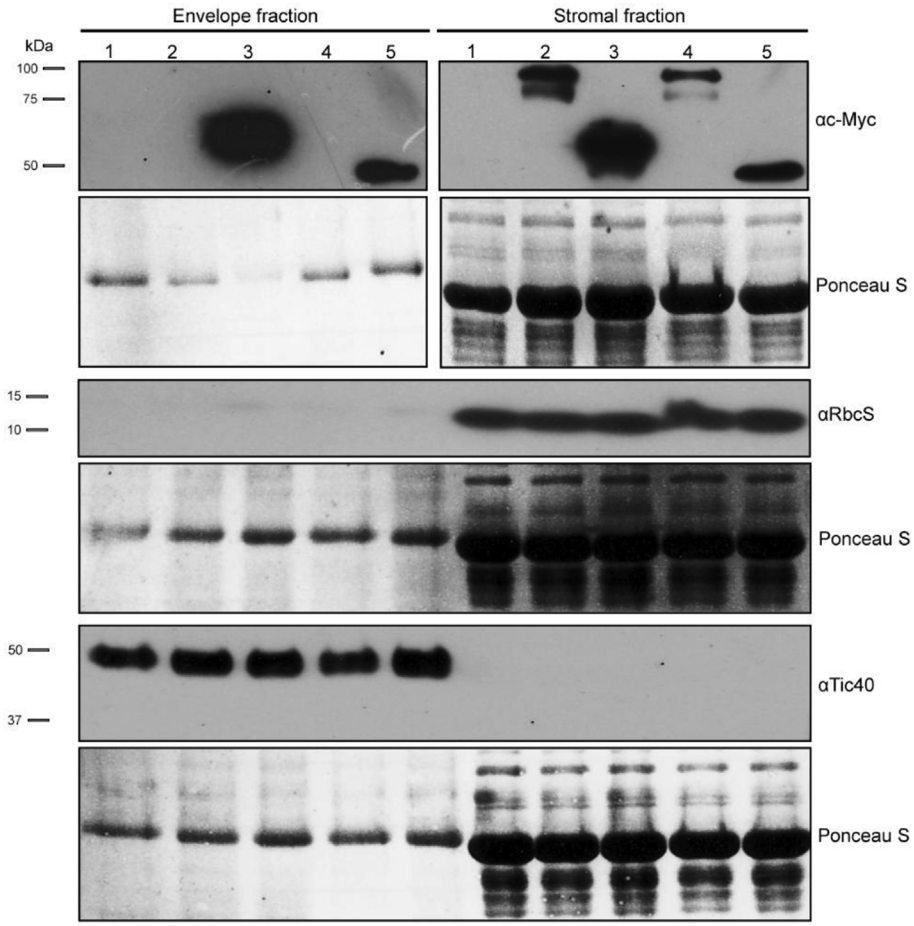

Fig. 4. Suborganellar localization of AtCGE1, AtCGE2 and cpHsc70–1 proteins. Western blot analysis of chloroplast proteins from purified chloroplast envelope and stroma from not agroinfiltrated leaves (lane 1) or leaves agroinfiltrated with *pNE::CPHSC70-1* (lanes 2 and 4), *pNE::CGE1* (lane 3), and *pNE::CGE2* (lane 5). Immunodetection of the c-Myc tagged AtCGE1, AtCGE2 and cpHsc70-1 protein fusions (αc-Myc), RbcS (αRbcS), and Tic40 (αTic40) proteins in the suborganellar samples is shown. The Ponceau S staining of the protein-containing membranes is shown as loading control. Molecular weight marker (kDa) is shown at the left. αc-Myc western-blots were performed on independent protein membranes.

(envelope protein marker) confirmed that no cross-contamination between the suborganellar fractions existed in the samples. This information corroborates the confocal microscopy data (Fig. 3) and demonstrates the co-localization between AtCGEs and cpHsc70-1 in the chloroplast stroma, supporting the hypothesis of a common function for these proteins.

2.4. A. thaliana CGEs interact with cpHsc70-1 in vivo

To analyze the existence of a physical interaction between the AtCGEs and the cpHsc70-1 chaperone *in vivo,* BiFC (Bimolecular Fluorescence Complementation) assays were performed. *N. benthamiana* leaves were transformed by agroinfiltration with the plasmids containing cpHsc70-1, AtCGE1 and AtCGE2 proteins fused to the N- (nYFP) and C-terminal (cYFP) regions of YFP protein (Fig. S2). Reciprocal co-transformation assays (i.e. cpHsc70-1-nYFP/AtCGE1-cYFP and cpHsc70-1-cYFP/AtCGE1-nYFP) were performed to corroborate the complementation of fluorescence. Fig. 5 shows that fused to nYFP or to cYFP, AtCGE1 directly interacts with cpHsc70-1 chaperone, as demonstrated by the presence of YFP fluorescence in the chloroplasts of transformed plant cells (Fig. 5A and B). Similar results were found for AtCGE2 and cpHsc70-1, the cells co-transformed with the nYFP and cYFP protein fusions displayed YFP fluorescence complementation in the chloroplast stroma (Fig. 5C and D). Furthermore, *N. benthamiana* protoplasts transformed with the individual translational fusions (i.e only AtCGE1-nYFP or AtCGE2-cYFP) were used as negative control for these experiments. Alternatively, using c-Myc and GFP-tagged proteins, we detected co-immunoprecipitation of AtCGE1 and AtCGE2 with cpHsc70-1 (Fig. S6), corroborating the interactions detected in the BiFC assays. Altogether, these observations demonstrate that the two AtCGEs form stable physical interactions with the cpHsc70-1 chaperone inside the chloroplasts *in vivo*.

2.5. A. thaliana CGEs form homo and heterodimers

It is known that bacterial GrpE interacts with DnaK as a homodimer, and this conformation is key for the regulation of the DnaK reaction cycle (Harrison et al., 1997). Dimerization has been reported for *C. reinhardtii* CGE1 (CrCGE1) (Schroda et al., 2001). To test the capacity of AtCGEs to form dimers, BiFC experiments were performed in *N. benthamiana* leaves transformed with the expression vectors containing AtCGE1 and AtCGE2 proteins fused to the cYFP and nYFP moieties of YFP protein (Fig. S2). Complementation of YFP fluorescence was detected in the chloroplasts of the cells transformed with the plasmids containing the fusions AtCGE1-cYFP and AtCGE1-nYFP (Fig. 6A), indicating that AtCGE1 protein forms homodimers *in vivo.* Similarly, YFP fluorescence was detected in the chloroplasts of the cells expressing the fusions AtCGE2-cYFP and AtCGE2-nYFP (Fig. 6B), demonstrating that AtCGE2 is capable of homodimerization *in vivo* too. Given that AtCGE1 and AtCGE2 belong to different clades of the CGE phylogenetic tree (Fig. S1), we were also interested in analyzing their ability to form heterodimers. YFP fluorescence was detected in the chloroplasts of the cells expressing the protein fusions AtCGE1-cYFP and AtCGE2-nYFP (Fig. 6C), and AtCGE2-cYFP and AtCGE1-nYFP (Fig. 6D), demonstrating that AtCGE1 and AtCGE2 can form heterodimers *in vivo*. Alternatively, using c-Myc and GFP-tagged proteins, we detected co-immunoprecipitation of AtCGE1 and AtCGE2 with AtCGE1, and AtCGE2 with AtCGE2 (Fig. S6), corroborating the interactions detected in the BiFC assays. In conclusion, these experiments support that the AtCGE1 and AtCGE2 proteins can form homodimers and heterodimers as well. Finally, as no data suggests the formation of cpHsc70-1 homodimers, protoplasts from *N. benthamiana* leaves transformed using the plasmids

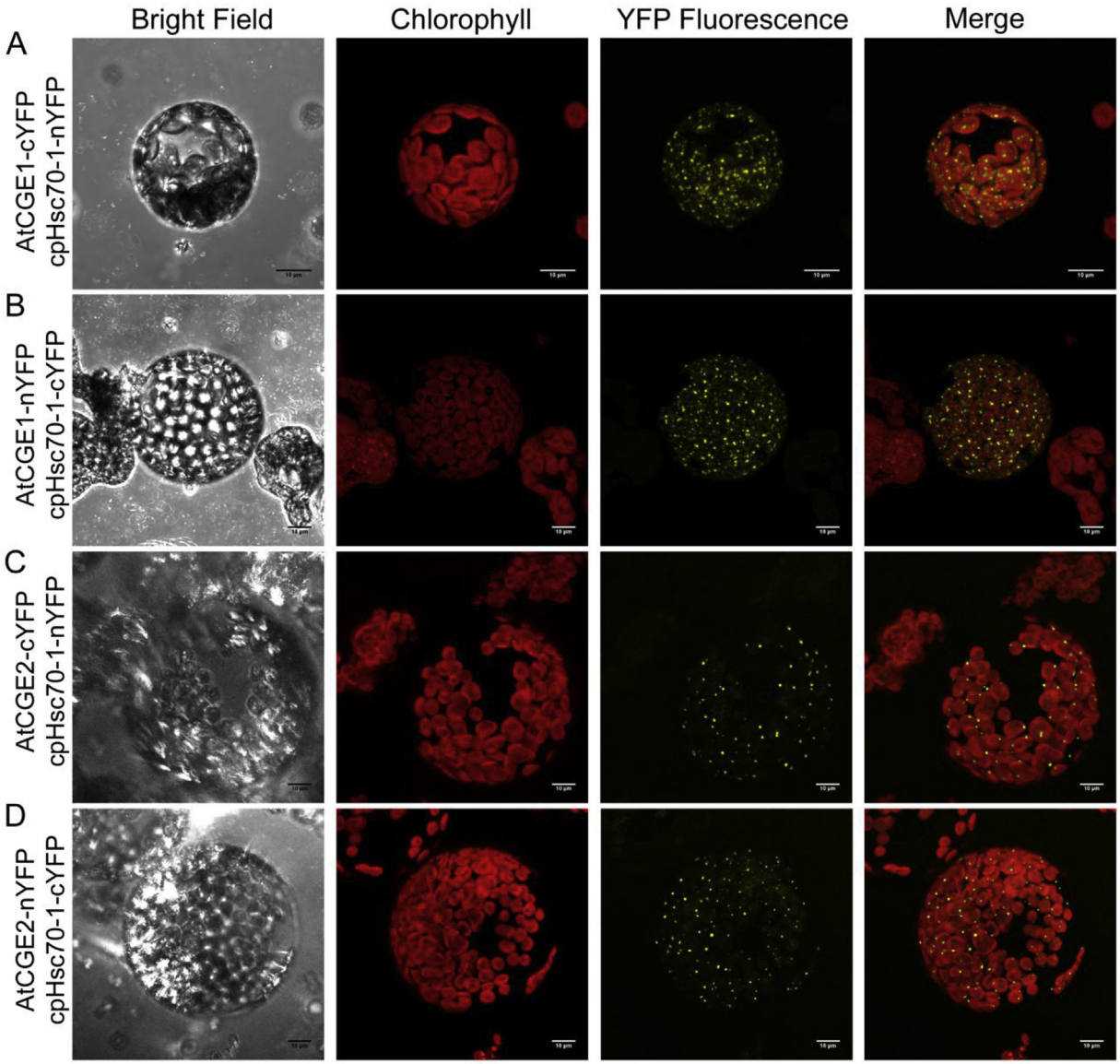

Fig. 5. *In vivo* interaction between AtCGEs and cpHsc70–1 proteins. Mesophyll protoplasts from *N. benthamiana* leaves co-expressing the translational fusions cpHsc70-1-nYFP and AtCGE1-cYFP (A), AtCGE1-nYFP and cpHsc70-1-cYFP (B), cpHsc70-1-nYFP and AtCGE2-cYFP (C), and AtCGE2-nYFP and cpHsc70-1-cYFP (D) are shown. Images corresponding to the bright field, chlorophyll fluorescence (Chlorophyll), reconstituted YFP fluorescence (YFP fluorescence), and the merge between the two fluorescence channels are shown in the indicated columns. Protoplasts were prepared 96 h after the agroinfiltration of the *N. benthamiana* leaves. Scale bars correspond to 10 μm. Negative controls are shown in Fig. S4.

containing the fusions cpHsc70-1-cYFP and cpHsc70-1-nYFP were used as a control, no fluorescence was detected in protoplasts from such leaves (Fig. 6E), indicating that the overexpression of proteins targeted to the chloroplast stroma does not result in unspecific interactions between the two moieties of YFP, validating the BiFC observations presented in Figs. 5 and 6.

2.6. CGE1 and CGE2 genes are differentially regulated in response to heat stress

In *E. coli*, *grpE* and *dnaK* genes are transcriptionally activated upon heat stress (Yura et al., 1993), a regulation that is conserved in the *CGE1* and *HSP70B* genes of *C. reinhardtii* but not in mitochondrial GrpEs from yeast or rat (Ang et al., 1986; Ikeda et al., 1994; Naylor et al., 1996; Schroda et al., 2001). To determine the transcriptional response of *AtCGE*s and *CPHSC70-1* genes to heat stress in seedlings, we first determined by Northern-blot the mRNA accumulation levels of *AtCGE1*, *AtCGE2* and *CPHSC70-1* under normal growth conditions in several developmental stages of wild-type seedlings (Fig. 7A and B). We found that *AtCGE1*, *AtCGE2* and *CPHSC70-1* genes are co-expressed at 8, 10, 12, and 14 days after germination (Fig. 7A and B). We also observed that the mRNA levels of *AtCGE2* and *CPHSC70-1* increase after 8 days of development and remain the same for the rest of the evaluated time points; furthermore, we found that the mRNA levels of *AtCGE1* are consistently downregulated 12 days after germination, but the initial levels are recovered later during development (Fig. 7A and B). Considering the downregulation of *AtCGE1* in 12-day-old seedlings, we decided to perform the heat stress experiments in 14-day-old seedlings exposed to 40 °C for 30, 60 and 90 min, and the mRNA levels of *AtCGE1*, *AtCGE2* and *CPHSC70-1* were analyzed by Northern blot. As shown in Fig. 7, *AtCGE1* transcript levels do not significantly change in response to heat treatment (Fig. 7C and D). In contrast, At*CGE2* mRNA levels decrease after 30 min of heat treatment (Fig. 7C and D). This response was like the observed in *DXS1*, a transcript that encodes a chloroplast-

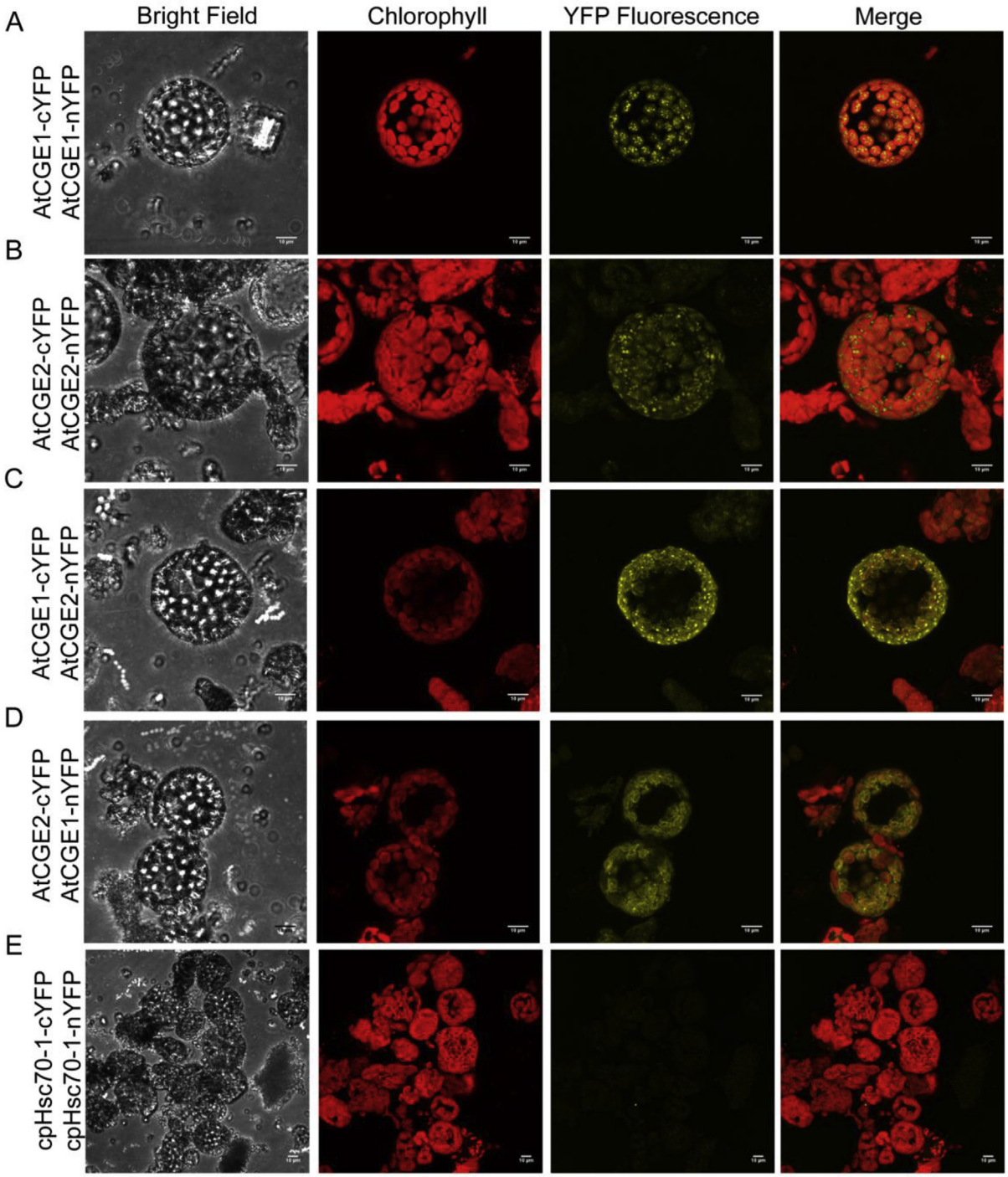

Fig. 6. *In vivo* determination of AtCGE1 and AtCGE2 dimer formation. Mesophyll protoplasts from *N. benthamiana* leaves co-expressing the translational fusions AtCGE1-nYFP and AtCGE1-cYFP (A), AtCGE2-nYFP and AtCGE2-cYFP (B), AtCGE2-nYFP and AtCGE1-cYFP (C), AtCGE1-nYFP and AtCGE2-cYFP (D), and cpHsc70-1-nYFP and cpHsc70-1-cYFP (E). Images corresponding to the bright field, chlorophyll fluorescence (Chlorophyll), reconstituted YFP fluorescence (YFP fluorescence), and the merge between the two fluorescence channels are shown in the indicated columns. Protoplasts were prepared 96 h after the agroinfiltration of the *N. benthamiana* leaves. Scale bars correspond to 10 μm.

localized protein with no chaperone function that was used as a control of the treatment (Fig. 7C and D). Finally, the abundance of *CPHSC70-1* mRNA shows downregulation after 30 and 60 min of heat stress but increases 90 min after the onset of the heat treatment (Fig. 7C and D); this response agrees with previous reports (Schroda et al., 2001). To our understanding, the fact that *AtCGE1* transcript levels do not change in response to heat stress, suggests that the AtCGE1 protein levels remain unchanged during the development of the stress response; at the same time, the downregulation of *AtCGE2* mRNA accumulation suggests that AtCGE2 protein levels decrease in response to heat stress. This hypothesis suggests that there are specific molecular mechanisms that differentially regulate the transcription or mRNA accumulation of the two AtCGEs; specifically, during the heat stress response, these mechanisms increase the AtCGE1 to AtCGE2 ratio, favoring the interactions between AtCGE1 and cpHsc70-1. These data suggest that AtCGE1 is the major AtCGE involved in the chloroplast's response to heat stress,

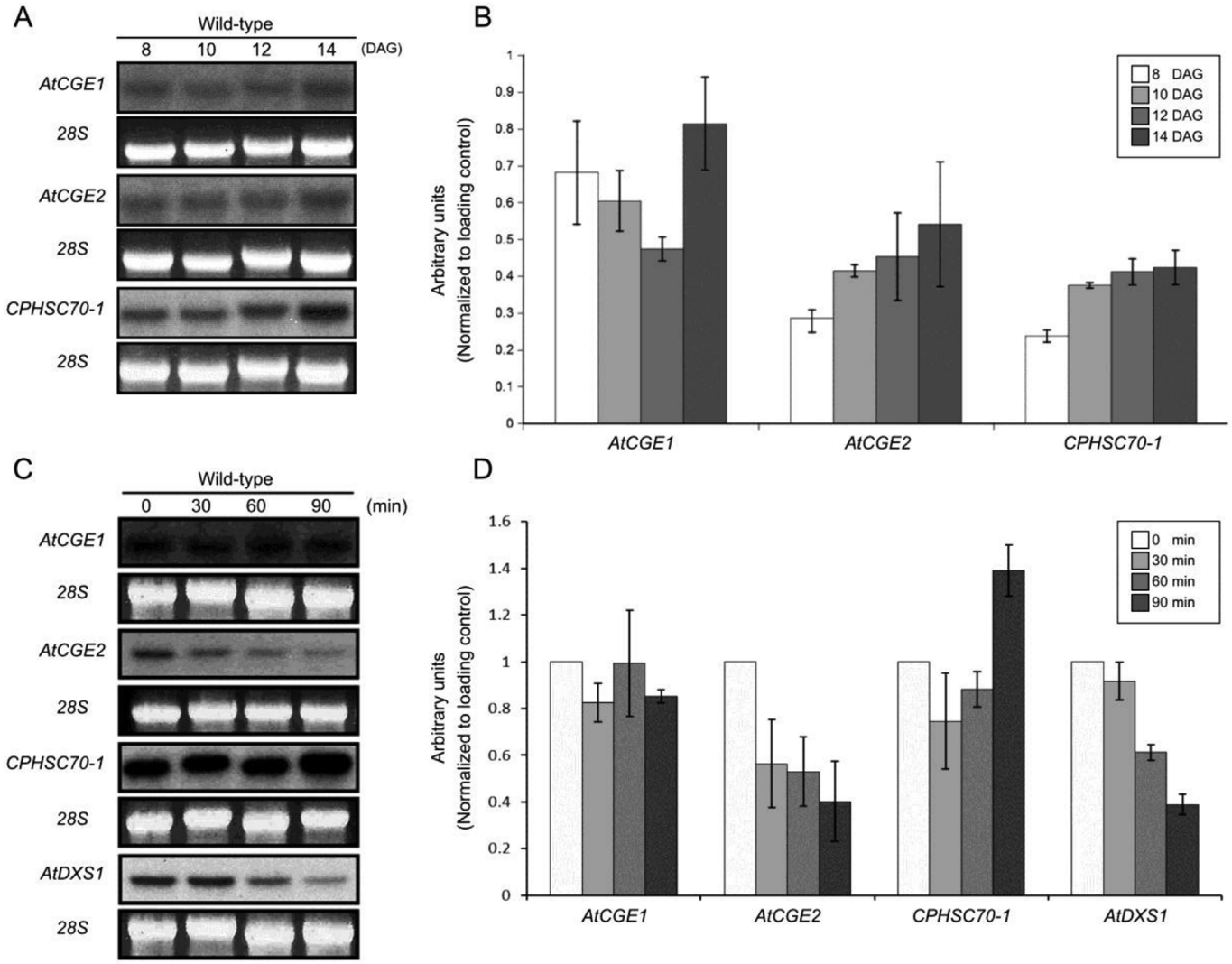

Fig. 7. Expression analysis of *AtCGE1*, *AtCGE2,* and *cpHsc70-1*. Northern blot hybridization of *AtCGE1*, *AtCGE2* and *CPHSC70-1* transcripts in four stages of seedling development (A), and the corresponding densitometry analysis is shown (B). Northern blot hybridization of *AtCGE1*, *AtCGE2*, *CPHSC70-1* and *DXS1* transcripts from wild-type seedlings after 0, 30, 60, and 90 min of heat stress(C). Densitometry analysis of the northern-blot data is shown considering 0 min as a reference (D). For each condition10 μg of total RNA were loaded and the ethidium bromide staining of the rRNA 28S is shown as a loading control. The DNA probes used are shown in Fig. S3. Error bars represent the standard error calculated from three independent experiments.

while AtCGE2 might be involved in a different biological process. However, the post-transcriptional regulation that controls the abundance of AtCGE proteins under heat stress remains to be analyzed.

2.7. *cge1 mutant plants have distinctive phenotypes*

To further explore the physiological roles of AtCGEs, we performed a phenotypic characterization of mutant plants for *AtCGE1*, and *CPHSC70-1* genes. As previously described, homozygous T-DNA insertion mutants in the *AtCGE1* gene (*emb1241-1* and *emb1241-2* mutants) are embryo-lethal (Meinke et al., 2008), preventing the phenotypic characterization of such plants. Thus, we analyzed the available heterozygote mutant lines *emb1241-1(±)*, *emb1241-2(±)*, and *cge2-1(±)*, and the homozygous mutant *Dcphsc70-1* (Fig. S3). The pigment-content analysis in these mutants showed a significant decrease in the content of chlorophyll *b* (chl *b*) in *Dcphsc70-1* and *emb1241-2(±)* mutant lines (Fig. 8A and Table S3). In contrast, no significant differences in pigment content were found in the *emb1241-1(±)* plants (Fig. 8A and Table S3). These results indicate the presence of alterations in the photosynthetic apparatus of *emb1241-2(±)* and *Dcphsc70-1* plants.

To support these findings, the accumulation of the photosystem I psaD1 and photosystem II D1 reaction center proteins was analyzed by Western blot in *emb1241-2(±)* and *Dcphsc70-1* plants. In Fig. 8B, we observed a higher accumulation of psaD1 and D1 in *emb1241-2(±)* and *Dcphsc70-1* mutants than in the wild-type plants (Fig. 8B), suggesting that the stoichiometry of the reaction centers or other parts of the photosynthetic apparatus might be altered in these plants. Using BN-PAGE, the accumulation of photosynthetic complexes was analyzed in *emb1241-2(±)* and *Dcphsc70-1* mutants. It was observed that both *emb1241-2(±)* and *Dcphsc70-1* accumulate lower levels of the functional oligomers of LHCII than the wild-type plants (Fig. 8C). Accordingly, the levels of LHCII monomer were higher in the *emb1241-2(±)* and *Dcphsc70-1* than in the wild-type plants (Fig. 8C). No significant differences in the abundance of the other major complexes (PSI and PSII) resolved in the gel were detected. These results suggest that cpHsc70-1 and AtCGE1 protein have a role in the proper oligomerization of the LHCII complex.

3. Discussion

Protein function largely depends on the protein's ability to interact

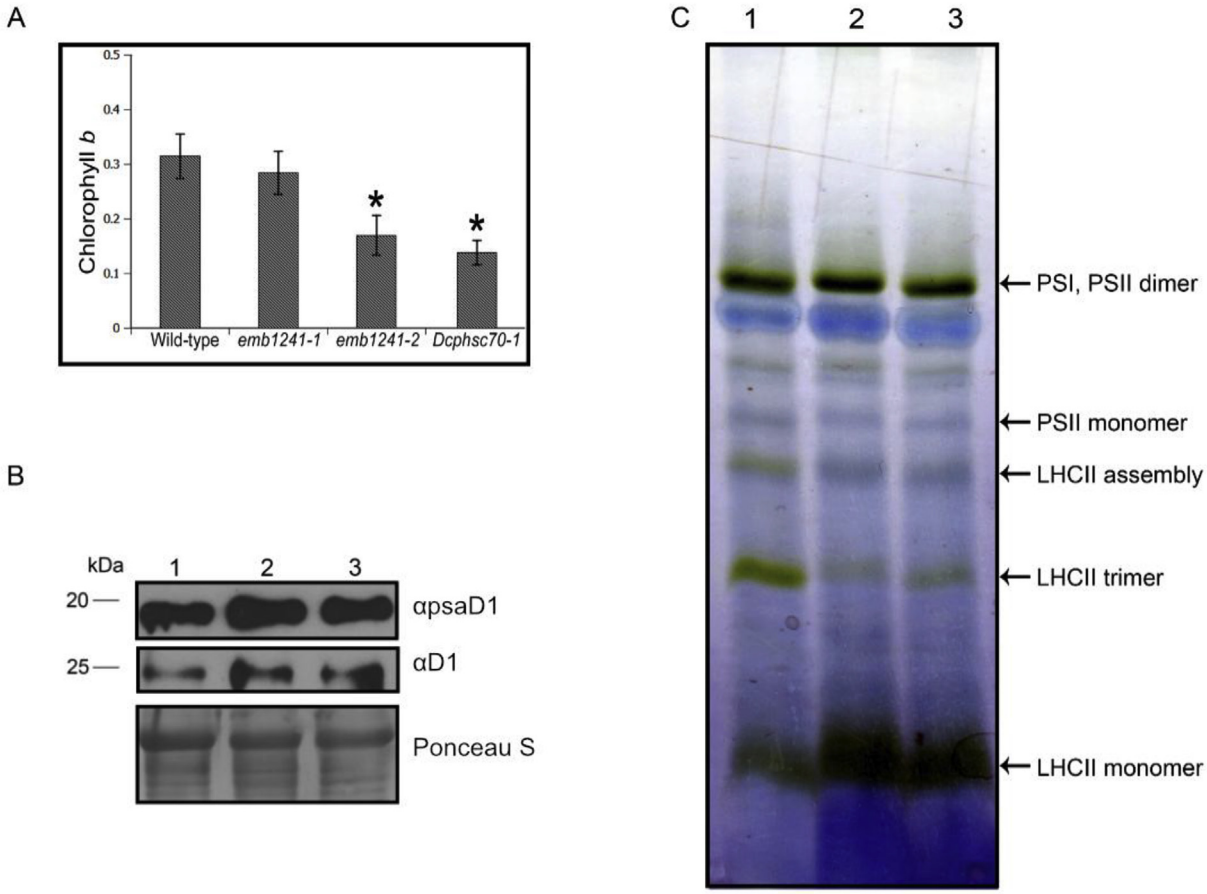

Fig. 8. Biochemical phenotype of *emb1241 (±)* and *Dcphsc70-1* mutants. The Chlorophyll *b* accumulation in wild-type, *emb1241-1 (±)*, *emb1241-2 (±)*, and *Dcphsc70-1* plants is shown (A). The error bars represent the standard error, the symbol (*) over the bars represent statistically significant differences calculated in a one-way analysis of variance with a significance level of $p<0.05$. The Immunodetection of psaD1 and D1 proteins (B) in total protein extracted from wild-type (1), *emb1241-2 (±)* (2), *and Dcphsc70-1* (3) adult plants is shown. The Ponceau S staining of the protein-containing membranes is shown as a loading control, molecular weight marker (in kDa) is shown at the left. Blue native-PAGE of total leaf protein (C) from wild-type (1), *emb1241-2 (±)* (2), and *Dcphsc70-1* (3) plants. Arrows point to the bands corresponding to the supramolecular complexes visible in the samples. (For interpretation of the references to colour in this figure legend, the reader is referred to the Web version of this article.)

with specific molecular partners to regulate aspects like folding, localization, and degradation; the most well-known protein partners are the chaperones. Chloroplastic chaperones of the Hsp70 family are known to be involved in protein import into the chloroplast and the formation of protein oligomers, and to have roles in cellular and physiological traits such as thylakoid biogenesis and thermotolerance (Schroda et al., 2001; Liu et al., 2007; Su and Li, 2008; Shi and Theg, 2010; Su and Li, 2010). It is known that Hsp70-family proteins work together with DnaJ and GrpE proteins (Mayer, 2010). In the plastids of land plants, it has been demonstrated that chloroplastic DnaJ proteins have roles in the homeostasis of proteins and PSII function (Pulido et al., 2013; Kong et al., 2013). However, the role that GrpE proteins play in the chloroplasts of higher plants has not been analyzed in detail.

Through a phylogenetic analysis, we identified the chloroplastic protein homologues of the bacterial GrpE protein in 61 land plant species, in accordance to previous reports we found two CGEs in *A. thaliana* that were named AtCGE1 and AtCGE2 (Schroda et al., 2001; Shi and Theg, 2010). Using a genetic complementation assay, we established the activity of the CGEs from *A. thaliana in vivo*. Due to the knockout of the *grpE* gene, the *E. coli* mutant strain OD212 has growth defects under heat stress conditions. Here we found that transformation with the coding regions of *AtCGE1* and *AtCGE2* genes can rescue the defective-growth phenotype of the *E. coli* strain OD212 at high temperatures. However, the complementation shown by the cells transformed with the *AtCGEs* is partial, since the heat-resistant phenotype conferred by the expression of the AtCGEs is weaker than the conferred by EcGrpE at 43 °C. This result might be due to differences in the amino acid positions important for the establishment of interactions with DnaK protein of AtCGE1 and AtCGE2, in comparison to the bacterial GrpE. It is known that mutation of six amino acid positions in the bacterial GrpE protein negatively affects the interaction with DnaK (Harrison et al., 1997; Gelinas et al., 2003, 2004); three of the six mentioned positions are conserved between GrpE and CGEs (R73, R183, and V192). However, positions R74 and K82 in the GrpE sequence are substituted by K and S residues respectively in CGEs. It is possible that these amino acid substitutions generate interactions between AtCGEs and DnaK, that are not as stable at 43 °C as the interactions between DnaK and EcGrpE, suggesting that these substitutions are responsible for the partial complementation displayed by the AtCGEs. Furthermore, the amino acid residue corresponding to position 122 of GrpE is the only functionally-relevant position that is different between Type A and Type B CGEs; Type A CGEs (such as AtCGE2) conserve the G residue present in the bacterial GrpE, while Type B CGEs (such as AtCGE1) present an S residue substitution at the corresponding position. The conservation of G122 in Type A CGEs explains the improved complementation displayed by AtCGE2 at 43 °C, apparently this position makes AtCGE2 more similar to the bacterial GrpE and likely results in better DnaK binding in comparison to AtCGE1. These observations suggest that AtCGEs form stable interactions with DnaK to supplement for the lack of endogenous GrpE in *E. coli*. Similar

complementation has been shown for other eukaryotic GrpE functional orthologues, such as the *C. reinhardtii* CGE1 (CrCGE1) and the yeast mitochondrial protein Mge1p (Deloche and Georgopoulos, 1996; Schroda et al., 2001), indicating that the two AtCGEs are functional nucleotide exchange factors that can be considered functional orthologues of the bacterial GrpE.

In addition to the activity and the amino acid conservation, several aspects of the AtCGEs biology were investigated to find a correlation between CGEs and chloroplastic Hsp70s in higher plants, given the fact that there are not available specific αCGE antibodies against the CGEs from higher plants, our main experimental strategies are based on the expression of recombinant proteins in *N. benthamiana* leaves. Using GFP-tagged proteins, colocalization of the chloroplastic homolog of DnaK (cpHsc70-1) and the two AtCGEs was detected, indicating that the two AtCGEs are effectively targeted to the chloroplast. Additionally, our mRNA accumulation experiments showed that *AtCGE1*, *AtCGE2* and *CPHC70-1* genes are co-expressed during seedling development in *A. thaliana*, indicating a strong correlation between the AtCGEs and CPHSC70-1 at the transcriptional and posttranscriptional level. Accordingly, CrCGE1 and the chloroplastic Hsp70 HSP70B, have been shown to accumulate mainly in the chloroplast stroma, indicating that their activities are spatially coordinated in algae (Schroda et al., 2001). In contrast, the present work showed that c-Myc tagged AtCGE1 and AtCGE2 accumulate not only in the stroma but also at the envelope of chloroplasts. In these experiments, c-Myc tagged cpHsc70-1 was only detected in the stromal fraction of the plastids. However, AtCGEs do not display features of integral membrane proteins, thus their localization at the chloroplast envelope must be mediated by interactions with unknown membrane proteins with functions not related to chaperone activity, or that might serve as scaffold to mediate interaction with the cpHsc70-1. In chloroplasts, the stromal side of Tic40 protein has sequence homology to the Hip and Hop cochaperones that are known to bind and regulate the activities of Hsp70 and Hsp90 chaperones (Stahl et al., 1999; Chou et al., 2003; Bédard et al., 2007); this observation suggests that similar interacting proteins might work to regulate the interaction between AtCGEs and cpHsc70-1 at the chloroplast envelope. Additionally, the immunodetection of AtCGEs at the chloroplast envelope corroborates the fluorescence distribution displayed by the translational fusions AtCGEs-GFP, which (in addition to the stromal localization) show the formation of cumuli that resemble envelope deformations caused by the overaccumulation of envelope proteins (Breuers et al., 2012). Altogether, these data demonstrate that the AtCGEs have a dual suborganellar distribution that might be due to interactions with unknown membrane proteins.

BiFC and co-immunoprecipitation assays were performed to demonstrate the existence of direct interactions between CGEs and chloroplastic Hsp70s. These experiments demonstrate that AtCGE1 and AtCGE2 form stable physical interactions with cpHsc70-1 *in vivo* inside the chloroplasts, corroborating the information obtained in the GFP-tagging experiments. Previous work has demonstrated that dimerization of GrpE proteins is fundamental for the establishment of interactions with Hsp70 proteins in *E. coli* and *S. cerevisiae* (Deloche and Georgopoulos, 1996; Wu et al., 1996; Azem et al., 1997). Taking advantage of our genetic constructs for BiFC and GFP-tagged proteins, we showed that the two CGEs from *A. thaliana* can form homodimers *in vivo*, indicating that the interaction mechanism between AtCGEs and cpHsc70-1 might be like the described for *E. coli* and *S. cerevisiae* (Deloche and Georgopoulos, 1996; Wu et al., 1996; Azem et al., 1997). In addition, we found that AtCGE1 and AtCGE2 form heterodimers *in vivo*; however, the relevance to chaperone activity of the formation of such heterodimers remains to be addressed. Together, these results indicate that the chloroplastic GrpE proteins of *A. thaliana* have the specific traits needed to physically interact with cpHsc70-1 and that their biological roles might be functionally linked to the activity of cpHsc70-1.

The activity of DnaK and GrpE proteins has been linked to heat stress responses (Yura et al., 1993). In *C. reinhardtii*, increased accumulation of *HSP70B* transcript has been detected upon incubation at 40 °C (Schroda et al., 2001). However, the transcriptional response of *A. thaliana CPHSC70-1* to heat stress is not fully consistent, with some studies detecting upregulation (Suzuki et al., 2013) and others detecting downregulation (Sung et al., 2001) in response to heat stress. In this regard, the heat stress experiments performed in this study showed overaccumulation of the *CPHSC70-1* mRNA 90 min after the onset of the heat treatment, supporting the physiological data of Su and Li (2008) that suggested the involvement of cpHsc70-1 protein in the thermotolerance of *A. thaliana* seedlings. In *C. reinhardtii*, increased accumulation of *CrCGE1* transcript was found in response to heat stress (Schroda et al., 2001). In our experiments, no significant changes in the accumulation of *AtCGE1* mRNA were detected after the heat treatment, whereas downregulation of the *AtCGE2* transcript was found after the onset of the treatment. The transcriptional response of *AtCGE2* is commonly observed in genes not related to heat stress responses (Rizhsky et al., 2002; Echevarría-Zomeño et al., 2016; Jiang et al., 2017). Based on this transcriptional data, we hypothesized that AtCGE1 protein has a higher likelihood to have a function that is coordinated with cpHsc70-1 in the chloroplastic heat stress responses. Also, the data presented suggest that the two AtCGE proteins might have independent roles in chloroplast biology.

In the past, cpHsc70-1 protein activity has been linked to several biological roles, including thermotolerance, thylakoid biogenesis, protein import and photosystem II assembly (Yalovsky et al., 1992; Schroda et al., 1999; Liu et al., 2007; Su and Li, 2008; Shi and Theg, 2010; Su and Li, 2010). As stated before, Hsp70 proteins work together with DnaJ cochaperones. Accordingly, different DnaJ proteins have been found to have biological roles like those of cpHsc70-1; such as the essential oligomerization of VIPP1 protein during thylakoid biogenesis, and the formation of PSII dimers and PSII-LHCII supercomplexes (Liu et al., 2005, 2007; Chen et al., 2010). To investigate the existence of a shared role for AtCGEs and cpHsc70-1, the accumulation of photosynthetic pigments was determined in leaves of the plant lines *Dcphsc70-1*, and the two alleles of *AtCGE1 emb1241-1(±)* and *emb1241-2(±)*. Such analysis detected a decrease in the content of chlorophyll *b* in the *Dcphsc70-1*, *emb1241-1(±)*, and *emb1241-2(±)* plant lines. As the biochemical phenotype is stronger in *emb1241-2(±)* than in *emb1241-1(±)*, only *emb1241-2(±)* plants were used for further analysis. In photosynthetic organisms, chlorophyll *b* is mainly associated with the LHCII complex of PSII (Green and Durnford, 1996; Kitajima and Hogan, 2003; Mascia et al., 2017). In agreement, the BN-PAGE analysis showed that the intensity of the protein bands corresponding to the LHCII trimer and the LHCII assembly from the *emb1241-2(±)* and *Dcphsc70-1* mutants, is reduced in comparison to the intensity of the corresponding bands in wild-type plants. In contrast, the abundance of the band corresponding to the monomeric state of the LHCII is increased in both mutants compared to the wild-type. This observation indicates that similar to what is observed for cpHsc70-1, the AtCGE1 protein is necessary for the correct assembling of the supramolecular organization of the LHCII complex, further supporting that the activity of AtCGE1 is functionally linked to that of cpHsc70-1 in *A. thaliana*.

As reported before, mutation of *CGE1* causes defects that result in the stunning of embryo development at the preglobular stage (Meinke et al., 2008). The fact that homozygous mutants for *AtCGE1* are embryo-lethal indicates that AtCGE2 protein is not able to supplement the absence of AtCGE1 protein. Furthermore, the phylogenetic analysis performed here shows that 35 plant species contain both Type A and Type B CGEs, while 26 species contain only one type of CGE protein (11 species have Type A and 15 species have Type B). These observations indicate that either type of CGE can perform all the functions of the two types of CGEs in the species that have only one type of CGE protein, a phenomenon that does not happen in the plant species that have the two types of CGEs, such as *A. thaliana*. This hypothesis suggests that

CGEs from species containing only one type of CGE must have different biochemical or molecular properties compared to CGEs from two type-containing species, that enables them to carry out the entire set of biological functions associated to CGE activity. These fundamental regulatory aspects of CGE biology will be investigated in detail in future research. Finally, the fact that the two AtCGEs are functional nucleotide-exchange factors that establish direct physical interactions with cpHsc70-1, suggests that despite their different biological roles, the two AtCGEs exert their functions through the enhancement of the activity of Hsp70 chaperones.

In conclusion, AtCGE1 and AtCGE2 proteins are the chloroplastic functional orthologues of the bacterial GrpE protein, they physically interact with cpHsc70-1 and mediate independent biological processes. We have evidence that suggests the involvement of AtCGE1, but not AtCGE2, in the homeostasis of LHCII functional oligomers.

4. Materials and methods

4.1. Plant material and growth conditions

Nicotiana benthamiana plants were cultured for 6 weeks in Metro-Mix 300 (Sun Gro Horticulture, USA) substrate supplemented with a controlled-release fertilizer (Osmocote Smart-release, The Scotts Miracle-Gro Company, USA) at 26 °C in a 16h light:8h dark photoperiod. For the experiments involving aseptic culture of plants, seeds were surface sterilized by incubation in a solution of 1% (v/v) NaClO, and cultured *in vitro* on 1X GM agar plates [4.3 g/L Murashige and Skoog salts with Gamborg's B5 vitamins (Phytotechnology Laboratories, USA), 1% w/v sucrose and 0.8% (w/v) phytoagar] at 22 °C in a 16:8h light:dark photoperiod. The *A. thaliana* T-DNA insertion lines *emb1241-1* (CS16149), *emb1241-2* (CS24098), and *Dcphsc70-1* (CS860808) were obtained from the Arabidopsis Biological Resource Center (www.arabidopsis.org). Populations of 30 adult plants (30 days old) of the mutant lines, were PCR-screened (Table S1) and only T-DNA-carrying plants were used for further analysis.

4.2. In silico analysis

Chloroplast GrpE protein sequences were identified and retrieved using the UniProtKB (http://www.uniprot.org/help/uniprotkb) BLAST tool, using the *E. coli* GrpE protein sequence as a query against the Plants database. In total, 136 CGE protein sequences were sorted by the presence of putative N-terminal chloroplast transit peptide. Transit peptide prediction was performed using TargetP 1.1 (Emanuelsson et al., 2000), and the predicted transit peptides were manually removed from the protein sequences. The analysis involved 137 amino acid sequences (136 CGEs and the GrpE from *E. coli*) that were aligned using Clustal Omega (http://www.ebi.ac.uk/Tools/msa/clustalo/) (CGEs full alignment file), the alignment was processed using MEGA 7.0.18 tools (Sudhir et al., 2016). The evolutionary history was inferred using the Maximum Likelihood method based on the JTT matrix-based model (Jones et al., 1992), a discrete Gamma distribution was used to model evolutionary rate differences among sites [5 categories (+G, parameter = 1.3736)]. Less than 30% alignment gaps, missing data, and ambiguous bases were allowed at any position. The phylogenetic tree was drawn using FigTree v1.4 (http://tree.bio.ed.ac.uk/software/figtree/). CGEs were sorted into Type A (48 sequences) and Type B (78 sequences) based on the information from the phylogenetic tree. Motif discovery was performed using the DREME tool from the MEME-suite (Bailey, 2011) fed with Type A or Type B sequences.

4.3. Gene cloning and plasmid construction

The *A. thaliana CGE1* (At5g17710), *CGE2* (At1g36390) and *CPHSC70-1* (At4g24280), and the bacterial *EcgrpE* (NC_000913.3) coding regions (CDS) were amplified by PCR using specific oligonucleotides to obtain the full CDS or to delete the transit peptides (Table S1). Entry vectors for Gateway cloning were generated by either recombination into pDONR™/Zeo donor vector or by directional cloning into pENTR/D-TOPO® entry vector. The expression plasmids (Fig. S2) were generated by LR clonase II-mediated (Invitrogen, USA) recombination of the entry vectors containing the coding regions of interest and destination vectors pDEST14 (*pD14*), pDEST22 (*pD22*), pDEST32 (*pD32*), pEarleyGate103 (*pEG*), pSPYCE (*pCE*), and pSPYNE (*pNE*). The expression plasmids constructed using *pEG*, *pCE*, and *pNE* were transferred to *Agrobacterium tumefaciens* C58C1 cells, individual clones were used for plant agroinfiltration.

4.4. E. coli complementation assay

The *E. coli* strain OD212 (*dnaK332 ΔgrpE::Ω-cam*^{R}) (Deloche et al., 1997) was transformed with *pD14::ΔCGE1, pD14::ΔCGE2, pD14::EcgrpE* and *pD14::ΔccdB* plasmids (Fig. S2), the cells were cultured overnight at 25 °C in solid lysogeny broth (LB) media. Individual colonies were cultured overnight in liquid LB medium at 25 °C, 100 μL of these cultures were used to inoculate fresh medium and allowed to grow to an OD_{600nm} of 0.1. Serial dilutions were prepared and 5 μL drops were plated on solid LB medium. The inoculated plates were incubated for 20 h at either 25 °C, 37 °C or 43 °C. All the LB media was supplemented with ampicillin to a final concentration of 100 μg/mL. The complementation experiments were replicated at least three times.

4.5. Subcellular and suborganellar localization, and Bimolecular Fluorescence Complementation (BiFC)

The subcellular localization and the BiFC experiments were performed using agroinfiltrated *Nicotiana benthamiana* leaves. Subcellular localization was determined using translational fusions between the proteins of interest and GFP, while BiFC experiments were carried out using the split YFP system (Walter et al., 2004). The agroinfiltration of *N. benthamiana* leaves was performed using *A. tumefaciens* clones individually containing the plasmids *pBN::GFP* (Voinnet et al., 2000), *pEG::CGE1*, *pEG::CGE2*, or *pEG::CPHSC70-1* for the subcellular localization experiments, and the corresponding plasmid combinations *pCE::CGE1, pCE::CGE2*, *pCE::CPHSC70-1*, *pNE::CGE1*, *pNE::CGE2,* and *pNE::CPHSC70-1* for BiFC assays. All the agroinfiltration experiments included the helper *A. tumefaciens* p19 strain (Leuzinger et al., 2013). The bacterial strains were cultured at 30 °C overnight, harvested by centrifugation (1, 400 × *g*, 10 min), and resuspended in a solution of 10 mM $MgCl_2$. The bacterial cultures were diluted to a final OD_{600nm} of 1 in 10 mM $MgCl_2$. The samples were incubated at room temperature for 3 h in the presence of 5 μg/mL acetosyringone prior to plant inoculation. Leaves of 6 weeks-old *N. benthamiana* plants were infiltrated with the bacterial samples and cultured at 26 °C in a 16h light:8h dark cycle for 96 h prior to analysis. Protoplasts from the infiltrated leaves were obtained by enzymatic digestion of the cell wall. Leaf strips were incubated in enzymatic solution (0.5 M mannitol, 1% cellulase R-10, and 0.05% macerozyme R-10) for 3 h in the dark, at room temperature, and mild shaking (~30 rpm). After digestion, leaf debris was removed and protoplasts were analyzed. Chloroplasts and suborganellar fractions from infiltrated leaves were isolated according to the method described by Salvi et al., (2011). All the experiments described in this section were performed by triplicate.

4.6. Confocal microscopy

Confocal microscopy images of *N. benthamiana* leaf protoplast were obtained with an Olympus FV1000 microscope (Olympus, USA) using excitation lasers of 488 nm for GFP and 515 nm for YFP, chlorophyll fluorescence was captured using a 515 nm laser and a barrier filter BA655-755. Z projections were rendered using the Fiji software maximum intensity projection type (Schindelin et al., 2012).

4.7. Plant heat stress experiments and northern blot

A. thaliana (Col-0) seedlings were cultured for 8, 10, 12 and 14 days under normal growth as described before. Fourteen days old *A. thaliana* (Col-0) seedlings were exposed to heat stress by incubation at 40 °C for 30, 60 or 90 min. Total RNA was prepared from the seedlings using TRIzol (Ambion, Life Technologies, USA) reagent, following the manufacturer's protocol. For northern blot analyses, 10 μg of total RNA were fractionated in 1.5% (w/v) agarose gels under denaturating conditions [2% (v/v) formaldehyde] and transferred to Hybond-N^+ nylon membrane (GE Healthcare Bio-Sciences, UK). Specific DNA probes for each of the genes were isolated from the CDSs and encompass the regions shown in Fig. S3. The specific DNA probes were radiolabeled with α-$dCT^{32}P$ using the Megaprime DNA labeling system (GE Healthcare Bio-Sciences, UK), following the protocol provided by the manufacturer. Hybridization and washing of the RNA-containing membranes were performed under stringent conditions (55 °C and 0.0825 M Na^+). All the experiments described in this section were performed by triplicate.

4.8. Pigment quantitation

Photosynthetic pigments (chlorophyll *a*, chlorophyll *b*, and carotenes) of adult plants were extracted by overnight incubation of leaves in 80% acetone solution. The absorbance of the samples was measured at 663 nm, 646 nm, and 470 nm. Using the absorbance data, the concentration of pigments was calculated with the following equations (Lichtenthaler and Wellburn, 1983):

$$\text{Chlorophyll a (Ca)} = (12.21^*A_{663})\text{-}(2.81^* A_{646})$$

$$\text{Chlorophyll b (Cb)} = (20.13^* A_{646})\text{-}(5.03^* A_{663})$$

$$Carotenes = ((1000^* A_{470})\text{-}(3.27^*Ca)\text{-}(104^*Cb))/229$$

The statistical significance of the data was determined using a One-Way ANOVA calculator (http://www.socscistatistics.com/tests/anova/Default2.aspx), with a significance level of $p < 0.05$.

4.9. Protein analyses

The protein isolated from suborganellar fractions was precipitated by addition of Tris-EDTA [100 mM Tris, 10 mM EDTA, pH 8], 0.3% sodium deoxycholate and 72% Trichloroacetic acid (TCA) in a reagent to sample ratio of 1:5 (v/v), the samples were incubated on ice for 1 h. The protein was collected by centrifugation at 25, 000 × *g*, resuspended in 90% acetone and incubated overnight at 4 °C. The samples were centrifuged at 25, 000 × *g*, and the pellets were allowed to air-dry before resuspension in a minimal volume of 2X Laemmli buffer [65 mM Tris-HCl pH 6.8, 30% (v/v) glycerol, 2% (w/v) SDS, 0.01% (w/v) bromophenol blue, 355 mM 2-mercaptoethanol] (Laemmli, 1970). The protein samples (10–20 μL) were fractionated in denaturating 12% polyacrylamide gels, transferred to nitrocellulose blotting membrane (GE Healthcare Bio-Sciences, UK), and incubated in PBS-T buffer [137 mM NaCl, 2.7 mM KCl, 10 mM Na_2HPO_4, 1.8 mM KH_2PO_4, 0.1% (v/v) Triton X-100] supplemented with 0.5% (w/v) nonfat dry milk. For Western blot analysis, monoclonal primary antibodies αc-Myc (Sigma-Aldrich, Mexico) and αHA (Santa Cruz Biotechnology Inc, USA), and secondary antibodies αMouse-HRP (Thermo Fisher Scientific, USA) and αRabbit-HRP (Thermo Fisher Scientific, USA) were used. Detection of the recombinant proteins was performed using the Amersham ECL Prime Western blotting detection reagent kit (GE Healthcare Bio-Sciences, UK), following the manufacturer's instructions.

For the BN-PAGE analysis, total protein from wild-type, *emb1241-2*, and *DcpHsc70-1* mutants was extracted by incubation of frozen-pulverized leaf tissue with BN extraction buffer [70 mM Tris-HCl pH 7.5, 1 mM $MgCl_2$, 25 mM KCl, 5 mM EDTA pH 8, 0.25 mM Sucrose, 39.1 mM n-Dodecyl β-D-maltoside], supplemented with the cOmplete™ protease inhibitor cocktail as indicated by the manufacturer (Sigma-Aldrich, Mexico). Protein samples were subjected to BN-PAGE in a 4%–14% acrylamide gradient, according to the protocol of Heinemeyer et al., (2007). Additionally, the BN-PAGE gels were destained by 10 consecutive washes of boiling-hot distilled water. All the experiments described in this section were performed at least three times.

Contribution

L. A. de Luna-Valdez: performed experiments, analyzed the results and wrote the manuscript.

C. I. Villaseñor-Salmerón: performed experiments.

A. A. Guevara-García: designed and supervised experiments, edited the manuscript and funded the research.

P. León-Mejía: edited the manuscript funded the research.

E. Cordoba: designed experiments and edited the manuscript.

R. Vera-Estrella: designed experiments and edited the manuscript.

Acknowledgements and Funding

The authors thank M.C. Andrés Saralegui and Dr. Arturo Pimentel from the Laboratorio Nacional de Microscopía Avanzada- Universidad Nacional Autónoma de México, for confocal microscopy services. Also, we thank Dr. Michael Schroda for the donation of the OD212 *E. coli* mutant strain. This work was supported by the PAPIIT-DGAPA-UNAM [grant numbers IN207214, IN210917 to AG and IN204617 to PL], also by the Consejo Nacional de Ciencia y Tecnología-Mexico [grant numbers CB2015-251848 to AG, CB2015-220534 and FC2016-96 to PL, and the student scholarship 240088 to LdL].

Appendix A. Supplementary data

Supplementary data to this article can be found online at https://doi.org/10.1016/j.plaphy.2019.03.027.

References

Ang, D., Chandrasekhar, G.N., Zylicz, M., Georgopoulos, C., 1986. Escherichia coli grpE gene codes for heat shock protein B25.3, essential for both lambda DNA replication at all temperatures and host growth at high temperature. J. Bacteriol. 167, 25–29.

Apuya, N.R., Yadegari, R., Fischer, R.L., Harada, J.J., Zimmerman, J.L., Goldberg, R.B., 2001. The Arabidopsis embryo mutant schlepperless has a defect in the chaperonin-60alpha gene. Plant Physiol. 126, 717–730.

Azem, A., Oppliger, W., Lustig, A., Jenö, P., Feifel, B., Schatz, G., Horst, M., 1997. The mitochondrial hsp70 chaperone system: effect of adenine nucleotides, peptide substrate, and mGrpE on the oligomeric state of mhsp70. J. Biol. Chem. 272, 20901–20906.

Bailey, T.L., 2011. DREME: motif discovery in transcription factor ChIP-seq data. Bioinformatics 27, 1653–1659.

Barraclough, R., Ellis, R.J., 1980. Protein synthesis in chloroplasts IX. Assembly of newly-synthesized large subunits into ribulose bisphosphate Carboxylase in isolated intact pea chloroplasts. Biochim. Biophys. Acta 608, 19–31.

Bédard, J., Kubis, S., Bimanadham, S., Jarvis, P., 2007. Functional similarity between the chloroplast translocon component, Tic40, and the human Co-chaperone, hsp70-interacting protein (Hip). J. Biol. Chem. 282, 21404–21414.

Breuers, F.K.H., Bräutigam, A., Geimer, S., Welzel, U.Y., Stefano, G., Renna, L., Brandizzi, F., Weber, A.P.M., 2012. Dynamic remodeling of the plastid envelope membranes a tool for chloroplast envelope in vivo localizations. Front. Plant Sci. 3, 7.

Cao, D., Froehlich, J.E., Zhang, H., Cheng, C.L., 2003. The chlorate-resistant and photomorphogenesis-defective mutant cr88 encodes a chloroplast-targeted HSP90. Plant J. 33, 107–118.

Chen, K.M., Holmström, M., Raksajit, W., Suorsa, M., Piippo, M., Aro, E.M., 2010. Small chloroplast-targeted DnaJ proteins are involved in optimization of photosynthetic reactions in Arabidopsis thaliana. BMC Plant Biol. 10, 43.

Chiu, C.C., Chen, L.J., Su, P.H., Li, Hm, 2013. Evolution of chloroplast J proteins. PLoS One. https://doi.org/10.1371/journal.pone.0070384.

Chou, M.L., Fitzpatrick, L.M., Tu, S.L., Budziszewski, G., Potter-Lewis, S., Akita, M., Levin, J.Z., Keegstra, K., Li, H.M., 2003. Tic40 a membrane-anchored Co-chaperone homolog in the chloroplast protein translocon. EMBO J. 22, 2970–2980.

Clarke, A.K., 2012. The chloroplast ATP-dependent clp protease in vascular plants - new dimensions and future challenges. Physiol. Plantarum 145, 235–244.

Constan, D., Froehlich, J.E., Rangarajan, S., Keegstra, K., 2004. A stromal Hsp100 protein is required for normal chloroplast development and function in Arabidopsis. Plant Physiol. 136, 3605–3615.

Deloche, O., Georgopoulos, C., 1996. Purification and biochemical properties of *Saccharomyces cerevisiae*'s Mge1p, the mitochondrial cochaperones of Ssc1p. J. Biol. Chem. 271, 23960–23966.
Deloche, O., Kelley, W.L., Georgopoulos, C., 1997. Structure-function analyses of the Ssc1p, Mdj1p, and Mge1p Saccharomyces cerevisiae mitochondrial proteins in Escherichia coli. J. Bacteriol. 179, 6066–6075.
Doyle, S.M., Wickner, S., 2009. Hsp104 and ClpB: protein disaggregating machines. Trends Biochem. Sci. 34, 40–48.
Echevarría-Zomeño, S., Fernández-Calvino, L., Castro-Sanz, A.B., López, J.A., Vázquez, J., Castellano, M.M., 2016. Dissecting the proteome dynamics of the early heat stress response leading to plant survival or death in Arabidopsis. Plant Cell Environ. 39, 1264–1278.
Emanuelsson, O., Nielsen, H., Brunak, S., von Heijne, G., 2000. Predicting subcellular localization of proteins based on their N-terminal amino acid sequence. J. Mol. Biol. 300, 1005–1016.
Farmaki, T., Sanmartin, M., Jimenez, P., Paneque, M., Sanz, C., Vancanneyt, G., Leon, J., Sanchez-Serrano, J.J., 2006. Differential distribution of the lipoxygenase pathway enzymes within potato chloroplasts. J. Exp. Bot. 58, 555–568.
Fink, A.L., 1999. Chaperone-mediated protein folding. Physiol. Rev. 79, 425–449.
Flores-Pérez, U., Jarvis, P., 2013. Molecular chaperone involvement in chloroplast protein import. Biochim. Biophys. Acta 1833, 332–340.
Gelinas, A.D., Toth, J., Bethoney, K.A., Langsetmo, K., Stafford, W.F., Harrison, C.J., 2003. Thermodynamic linkage in the GrpE nucleotide exchange factor, a molecular thermosensor. Biochemistry 42, 9050–9059.
Gelinas, A.D., Toth, J., Bethoney, K.A., Stafford, W.F., Harrison, C.J., 2004. Mutational analysis of the energetics of the GrpE.DnaK binding interface: equilibrium association constants by sedimentation velocity analytical ultracentrifugation. J. Mol. Biol. 33, 447–458.
Green, B.R., Durnford, D.G., 1996. The chlorophyll-carotenoid proteins of oxygenic photosynthesis. Annu. Rev. Plant Physiol. Plant Mol. Biol. 47, 685–714.
Harrison, C.J., Hayer-Hartl, M., Di, L.M., Hartl, F., Kuriyan, J., 1997. Crystal structure of the nucleotide exchange factor GrpE bound to the ATPase domain of the molecular chaperone DnaK. Science 276, 431–435.
Heide, H., Nordhues, A., Drepper, F., Nick, S., Schulz-Raffelt, M., Haehnel, W., Schroda, M., 2009. Application of quantitative immunoprecipitation combined with knockdown and cross-linking to Chlamydomonas reveals the presence of vesicle-inducing protein in plastids 1 in a common complex with chloroplast HSP90C. Proteomics 9, 3079–3089.
Heinemeyer, J., Lewejohann, D., Braun, H.P., 2007. Blue-native gel electrophoresis for the characterization of protein complexes in plants. Methods Mol. Biol. 355, 343–352.
Ikeda, E., Yoshida, S., Mitsuzawa, H., Uno, I., Toh-e, 1994. A. YGE1 is a yeast homologue of Escherichia coli GrpE and is required for maintenance of mitochondrial functions. FEBS (Fed. Eur. Biochem. Soc.) Lett. 339, 265–268.
Inoue, H., Li, M., Schnell, D.J., 2013. An essential role for chloroplast heat shock protein 90 (Hsp90C) in protein import into chloroplasts. Proc. Natl. Acad. Sci. Unit. States Am. 110, 3173–3178.
Jarvis, P., Kessler, F., 2014. Mechanisms of chloroplast protein import in plants. In: In: Theg, S., Wollman, F.A. (Eds.), Plastid Biology. Advances in Plant Biology, vol. 5. Springer, New York, pp. 241–270.
Jiang, J., Liu, X., Liu, C., Liu, G., Li, S., Wang, L., 2017. Integrating omics and alternative splicing reveals insights into grape response to high temperature. Plant Physiol. 173, 1502–1518.
Jones, D.T., Taylor, W.R., Thornton, J.M., 1992. The rapid generation of mutation data matrices from protein sequences. Bioinformatics 8, 275–282.
Kitajima, K., Hogan, K.P., 2003. Increases of chlorophyll a/b ratios during acclimation of tropical woody seedlings to nitrogen limitation and high light. Plant Cell Environ. 26, 857–865.
Kong, F., Deng, Y., Zhou, B., Wang, G., Wang, Y., Meng, Q., 2014. A chloroplast-targeted DnaJ protein contributes to maintenance of photosystem II under chilling stress. J. Exp. Bot. 65, 143–158.
Kovacheva, S., Bédard, J., Patel, R., Dudley, P., Twell, D., Ríos, G., Koncz, C., Jarvis, P., 2005. In vivo studies on the roles of Tic110, Tic40 and Hsp93 during chloroplast protein import. Plant J. 41, 412–428.
Kovacheva, S., Bédard, J., Wardle, A., Patel, R., Jarvis, P., 2007. Further in vivo studies on the role of the molecular chaperone Hsp93, in plastid protein import. Plant J. 50, 364–379.
Laemmli, U.K., 1970. Cleavage of structural proteins during the assembly of the head of bacteriophage T4. Nature 227, 680–685.
Leuzinger, K., Dent, M., Hurtado, J., Stahnke, J., Lai, H., Zhou, X., Chen, Q., 2013. Efficient agroinfiltration of plants for high-level transient expression of recombinant proteins. JoVE 77, 50521.
Lichtenthaler, H.K., Wellburn, A.R., 1983. Determinations of total carotenoids and chlorophylls a and b of leaf extracts in different solvents. Biochem. Soc. Trans. 11, 591–592.
Liu, C., Willmund, F., Whitelegge, J.P., Hawat, S., Knapp, B., Lodha, M., Schroda, M., 2005. J-domain protein CDJ2 and HSP70B are a plastidic chaperone pair that interacts with vesicle-inducing protein in plastids 1. Mol. Biol. Cell 16, 1165–1177.
Liu, C., Willmund, F., Golecki, J.R., Cacace, S., Heß, B., Markert, C., Schroda, M., 2007. The chloroplast HSP70B-CDJ2-CGE1 chaperones catalyse assembly and disassembly of VIPP1 oligomers in Chlamydomonas. Plant J. 50, 265–277.
Martin, W., Stoebe, B., Goremykin, V., Hapsmann, S., Hasegawa, M., Kowallik, K.V., 1998. Gene transfer to the nucleus and the evolution of chloroplasts. Nature 393, 162–165.
Mascia, F., Girolomoni, L., Alcocer, M.J.P., Bargigia, I., Perozeni, F., Cazzaniga, S., Cerullo, G., D'Andrea, C., Ballottar, M., 2017. Functional analysis of photosynthetic pigment binding complexes in the green alga *Haematococcus pluvialis* reveals distribution of astaxanthin in Photosystems. Sci. Rep. 7, 16319.
May, T., Soll, J., 2000. 14-3-3 proteins form a guidance complex with chloroplast precursor proteins in plants. Plant Cell 12, 53–63.
Mayer, M.P., 2010. Gymnastics of molecular chaperones. Mol. Cell 39, 321–331.
Meinke, D., Muralla, R., Sweeney, C., Dickerman, A., 2008. Identifying essential genes in Arabidopsis thaliana. Trends Plant Sci. 13, 483–491.
Naylor, D.J., Hoogenraad, N.J., Høj, P.B., 1996. Isolation and characterisation of a CDNA encoding rat mitochondrial GrpE a stress-inducible nucleotide-exchange factor of ubiquitous appearance in mammalian organs. FEBS (Fed. Eur. Biochem. Soc.) Lett. 396, 181–188.
Nelson, B.K., Cai, X., Nebenführ, A., 2007. A multicolored set of in vivo organelle markers for Co-localization studies in Arabidopsis and other plants. Plant J. 51, 1126–1136.
Olinares, P.D., Kim, J., van Wijk, K.J., 2011. The clp protease system; a central component of the chloroplast protease network. Biochim. Biophys. Acta 1807, 999–1011.
Paila, Y.D., Richardson, L.G.L., Schnell, D.J., 2015. New insights into the mechanism of chloroplast protein import and its integration with protein quality control organelle biogenesis and development. J. Mol. Biol. 427, 1038–1060.
Peng, L., Fukao, Y., Myouga, F., Motohashi, R., Shinozaki, K., Shikanai, T., 2011. A chaperonin subunit with unique structures is essential for folding of a specific substrate. PLoS Biol. https://doi.org/10.1371/journal.pbio.1001040.
Perello, C., Llamas, E., Burlat, V., Ortiz-Alcaide, M., Phillips, M.A., Pulido, P., Rodriguez-Concepcion, M., 2016. Differential subplastidial localization and turnover of enzymes involved in isoprenoid biosynthesis in chloroplasts. PLoS One. https://doi.org/10.1371/journal.pone.0150539.
Pratt, W.B., Toft, D.O., 2003. Regulation of signaling protein function and trafficking by the hsp90/hsp70-Based chaperone machinery. Exp. Biol. Med. 228, 111–133.
Pulido, P., Toledo-Ortiz, G., Phillips, M.A., Wright, L.P., Rodriguez-Concepcion, M., 2013. Arabidopsis J-protein J20 delivers the first enzyme of the plastidial isoprenoid pathway to protein quality control. Plant Cell 25, 4183–4194.
Qbadou, S., Becker, T., Mirus, O., Tews, I., Soll, J., Schleiff, E., 2006. The molecular chaperone Hsp90 delivers precursor proteins to the chloroplast import receptor Toc64. EMBO J. 25, 1836–1847.
Rial, D.V., Arakaki, A.K., Ceccarelli, E.A., 2000. Interaction of the targeting sequence of chloroplast precursors with Hsp70 molecular chaperones. Eur. J. Biochem. 267, 6239–6248.
Rizhsky, L., Liang, H., Mittler, R., 2002. The combined effect of drought stress and heat shock on gene expression in tobacco. Plant Physiol. 130, 1143–1151.
Salvi, D., Moyet, L., Seigneurin-Berny, D., Ferro, M., Joyard, J., Rolland, N., 2011. Preparation of envelope membrane fractions from Arabidopsis chloroplasts for proteomic analysis and other studies. In: Jarvis, R. (Ed.), Chloroplast Research in Arabidopsis. Humana Press, pp. 189–206.
Schindelin, J., Arganda-Carreras, I., Frise, E., et al., 2012. Fiji: an open-source platform for biological-image analysis. Nat. Methods 9, 676–682.
Schroda, M., Vallon, O., Wollman, F.A., Beck, C.F., 1999. A chloroplast-targeted heat shock protein 70 (HSP70) contributes to the photoprotection and repair of photosystem II during and after photoinhibition. Plant Cell 11, 1165–1178.
Schroda, M., Vallon, O., Whitelegge, J.P., Beck, C.F., Wollman, F.A., 2001. The chloroplastic GrpE homolog of Chlamydomonas: two isoforms generated by differential splicing. Plant Cell 13, 2823–2839.
Shi, L.X., Theg, S.M., 2010. A stromal heat shock protein 70 system functions in protein import into chloroplasts in the moss Physcomitrella patens. Plant Cell 22, 205–220.
Sjogren, L.L.E., Tanabe, N., Lymperopoulos, P., Khan, N.Z., Rodermel, S.R., Aronsson, H., Clarke, A.K., 2014. Quantitative analysis of the chloroplast molecular chaperone ClpC/hsp93 in Arabidopsis reveals new insights into its localization interaction with the clp proteolytic core, and functional importance. J. Biol. Chem. 289, 11318–11330.
Stahl, T., Glockmann, C., Soll, J., Heins, L., 1999. Tic40, a new old subunit of the chloroplast protein import translocon. J. Biol. Chem. 274, 37467–37472.
Su, P.H., Li, H.M., 2008. Arabidopsis stromal 70-KD heat shock proteins are essential for plant development and important for thermotolerance of germinating seeds. Plant Physiol. 146, 1231–1241.
Su, P.H., Li, H.M., 2010. Stromal Hsp70 is important for protein translocation into pea and Arabidopsis chloroplasts. Plant Cell 22, 1516–1531.
Sudhir, K., Stecher, G., Tamura, K., 2016. MEGA7: molecular evolutionary genetics analysis version 7.0 for bigger datasets. Mol. Biol. Evol. 33, 1870–1874.
Sung, D.Y., Vierling, E., Guy, C.L., 2001. Comprehensive expression profile Analysis of the Arabidopsis Hsp70 gene family. Plant Physiol. 126, 789–800.
Suzuki, N., Miller, G., Salazar, C., et al., 2013. Temporal-spatial interaction between reactive oxygen species and abscisic acid regulates rapid systemic acclimation in plants. Plant Cell 25, 353–3569.
Trösch, R., Mühlhaus, T., Schroda, M., Willmund, F., 2015. ATP-dependent molecular chaperones in plastids–more complex than expected. Biochim. Biophys. Acta 1847, 872–888.
Tsai, Y.C., Mueller-Cajar, O., Saschenbrecker, S., Hartl, F.U., Hayer-Hartl, M., 2012. Chaperonin cofactors, Cpn10 and Cpn20, of green algae and plants function as hetero-oligomeric ring complexes. J. Biol. Chem. 287, 20471–20481.
van Wijk, K.J., Baginsky, S., 2011. Plastid proteomics in higher plants: current state and future goals. Plant Physiol. 155, 1578–1588.
Villarejo, A., Burén, S., Larsson, S., et al., 2005. Evidence for a protein transported through the secretory pathway en route to the higher plant chloroplast. Nat. Cell Biol. 7, 1224–1231.
Voinnet, O., Lederer, C., Baulcombe, D.C., 2000. A viral movement protein prevents spread of the gene silencing signal in *Nicotiana benthamiana*. Cell 103, 157–167.
Walter, M., Chaban, C., SchützenK, et al., 2004. Visualization of protein interactions in living plant cells using bimolecular fluorescence complementation. Plant J. 40,

428–438.
Willmund, F., Muhlhaus, T., Wojciechowska, M., Schroda, M., 2007. The NH2-terminal domain of the chloroplast GrpE homolog CGE1 is required for dimerization and co-chaperone function in vivo. J. Biol. Chem. 282, 11317–11328.
Wu, B., Ang, D., Snavely, M., Georgopoulos, C., 1996. Structure-function analysis of the *Escherichia coli* GrpE heat shock protein. EMBO J. 15, 4806–4816.
Yalovsky, S., Paulsen, H., Michaeli, D., Chitnis, P.R., Nechushtai, R., 1992. Involvement of a chloroplast HSP70 heat shock protein in the integration of a protein (Light-Harvesting complex protein precursor) into the thylakoid membrane. Proceedings of the National Academy of Sciences USA 89, 5616–5619.
Yura, T., Nagai, H., Mori, H., 1993. Regulation of the heat-shock response in bacteria. Annu. Rev. Microbiol. 47, 321–350.